Development of Banded Structure in a Numerically Simulated Hurricane

MUKUT B. MATHUR

National Meteorological Center, NWS, NOAA, Washington, D. C. 20023

(Manuscript received 2 May 1974, in revised form 15 October 1974)

ABSTRACT

The developments of the propagating and the stationary bands in a three-dimensional model of a hurricane (Isbell, 1964) are investigated. Propagating bands in the vertical motion fields in the middle and the upper troposphere form in the regions of strong heating in the upper troposphere and weak cooling in the middle troposphere. The structures of the wind, temperature and pressure fields in these bands are similar to those observed in the outer radar bands of hurricanes. Strong, nearly stationary bands form close to the center in the intense storm stage.

Results of two experiments, one (M1) in which the so-called nonconvective release of latent heat in the upper troposphere is included and the other (M2) in which this heating is not incorporated, are compared. Convective release of latent heat is included in both experiments. The stationary bands which form in M1, also develop in M2. The propagating bands which form in M1, however, do not develop in M2. The rate of intensification of the simulated storm in M1 is nearly the same as observed in Isbell; it is, however, significantly weaker in M2. It is shown that the inclusion of nonconvective release of latent heat in M1 enhances the upper tropospheric outflow which induces strong zones of convergence in the boundary layer. The resulting increase in the upward motion at the top of the boundary layer augments the convective release of latent heat and leads to a rapid intensification of the disturbance.

1. Introduction

In earlier papers, Mathur (1972, 1974) presented the results of a 96 h integration of a fine-mesh, multiple-grid, primitive equation model which simulated the development of an actual hurricane (Isbell, 1964). The movement and the rate of intensification of the initial depression (data derived from actual observations) into a hurricane simulated by the model agreed fairly well with those observed during the formation of hurricane Isbell. Features of hurricanes which were realistically simulated included organized bands in the vertical motion fields close to and surrounding the center, downward motion and weak horizontal winds in the eye, zones of convergence in the boundary layer, cyclonic outflow in the upper troposphere, and the central warm core.

Two types of bands, propagating and stationary, form in the experiment (hereafter referred to as M1) described by Mathur (1974). The propagating bands form in the regions where a large release of latent heat takes place in the upper troposphere compared to that in the middle troposphere, so that the net heating takes place in the upper troposphere and weak cooling in the middle troposphere. When the cooling due to vertical advection exceeds condensational heating in the upper troposphere, these bands dissipate. The structure of these bands is similar to the outer radar bands in hurricanes. Features like the zone of convergence in the boundary layer, mesotrough of low pressure, fall in temperature, changes in the wind speed and the direction, which are observed in the outer radar bands of hurricanes, are well simulated by the model.

The propagating bands do not form in an experiment (M2) in which the so-called nonconvective release of latent heat is not incorporated. The stationary bands close to the center form at nearly the same location in both experiments, suggesting that these bands are associated with the convective release of latent heat. Although the propagating bands form only when the nonconvective release of latent heat is included, the convective release of latent heat in these bands is several times larger than the nonconvective release of latent heat.

The rate of intensification of the disturbance in M1 agrees fairly well with the observations in Isbell; the rate of intensification is significantly weaker in M2. This difference in the rates of intensification suggests that both the inclusion of the nonconvective release of latent heat and the simulation of the propagating bands, in which large convective release of latent heat takes place, are of considerable importance for the proper numerical prediction of tropical disturbances. The convective release of latent heat in M1 is very large compared to the nonconvective release of latent heat. The precipitation in the simulated disturbance is therefore largely convective.

2. Brief review of the model

The primitive equations with pressure (p) as the vertical coordinate are integrated using a quasi-Lagrangian advective scheme (Mathur, 1970). The variables are staggered in the vertical. The eastward (u) and northward (v) components of the wind and the geopotential (z) are defined at 1000, 900, 550 and 200 mb. The potential temperature (θ), mixing ratio (q), and the vertical motion (ω) appear at the intermediate levels (950, 725 and 375 mb). The vertical motion is also calculated at 1000 mb.

The sensible and latent heat fluxes from the sea to the boundary layer air, surface friction, the variation of the Coriolis parameter with latitude, and the convective and the nonconvective release of latent heat are incorporated in the model.

The effects of the surface friction are included in the equation of motion at 1000 mb. The vertical stress terms at this level are

$$\left.\begin{aligned} F_{uz} &= -C_D\rho|\mathbf{V}_0|u_0 g/\Delta p \\ F_{vz} &= -C_D\rho|\mathbf{V}_0|v_0 g/\Delta p \end{aligned}\right\},$$

where ρ is the density of air, g the acceleration due to gravity, and the subscript 0 indicates conditions at 1000 mb. The drag coefficient C_D is assumed to have a constant value of 0.0025.

The predictive equation for the potential temperatures in the quasi-Lagrangian advective scheme is

$$\frac{D\theta}{Dt}=\frac{H}{c_p}\left(\frac{1000}{p}\right)^{R/c_p}-\omega\frac{\partial\theta}{\partial p}+\text{Diffusion}, \qquad (1)$$

where H is rate of heating and

$$\frac{D}{Dt}=\frac{\partial}{\partial t}+u\frac{\partial}{\partial x}+v\frac{\partial}{\partial y}.$$

The release of latent heat in the middle and the upper troposphere due to the convective scale motions (Hcu) is:

$$\mathrm{Hcu}(p)=\left\{\frac{-\omega_B q_B}{\int_{p_T}^{p_B}\frac{c_p}{L}(T_s-T)dp+\int_{p_T}^{p_B}(q_s-q)dp}\right\}\times c_p[T_s(p)-T(p)], \qquad (2)$$

provided that $T_s>T$ and $\omega_B<0$.

The subscripts B, T and s denote the top of the boundary layer, top of the convective cloud, and conditions within the cloud, respectively.

Eq. (2) relates the convective release of latent heat to the vertical motion at the top of the boundary layer. The convergence in the boundary layer in the present unbalanced model is not entirely due to friction; it can also be caused by allobaric effect [see the discussion in Syono and Yamasaki (1968)]. The parameterization of convective release of latent heat represented by Eq. (2) is otherwise a simple formulation of the conditional instability of the second kind (CISK) proposed by Charney and Eliassen (1964).

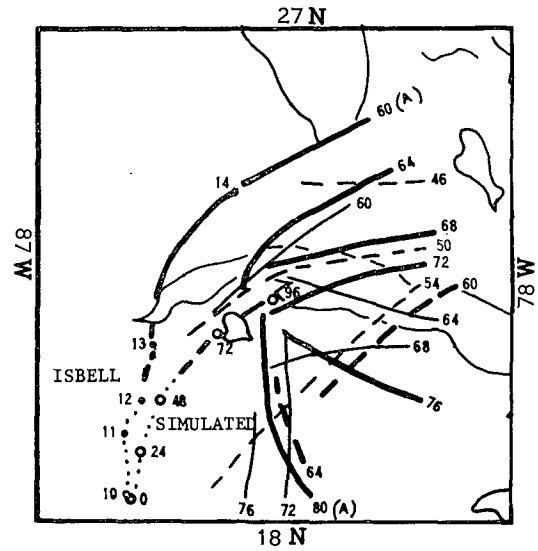

FIG. 1. Track of a few bands in the vertical motion field at 375 mb in experiment M1. Tracks of the simulated disturbance in M1 and Isbell (position at 1200 GMT) are also shown: depression, dotted lines; storm, dashed lines; hurricane, solid line.

The lower and the middle tropospheres in the tropics are generally conditionally unstable. This instability is also observed in the regions of disturbed weather. Reed and Recker (1971) suggested that the layer clouds in sufficient quantities do not exist in the tropical wave disturbances below 300 mb. The so-called nonconvective release of latent heat (HST) associated with the large-scale ascent of moist air is, therefore, included in the present model only in the upper troposphere:

$$\mathrm{HST}=-L\omega\frac{\partial q_s}{\partial p}, \qquad (3)$$

provided $\omega<0$ and relative humidity $>95\%$.

The domain of integration covers the Gulf of Mexico from 14 to 30°N, with the eastern and western boundaries being 76 and 92°W, respectively. A multiple-grid system, which allows a higher resolution near the center of the disturbance and the mutual interaction between the areas (scales) covered by different grid sizes, is utilized. In the area bound by latitudes 18 and 26°N and longitudes 80 and 88°W, the grid distance is approximately 37 km (fine mesh). Outside this area, the grid distance is approximately 74 km (coarse mesh). The area of the fine mesh is chosen so that the track of Isbell in the real atmosphere is located in the fine-mesh region throughout the integration period (96 h).

For a complete description of the model, see Mathur (1972).

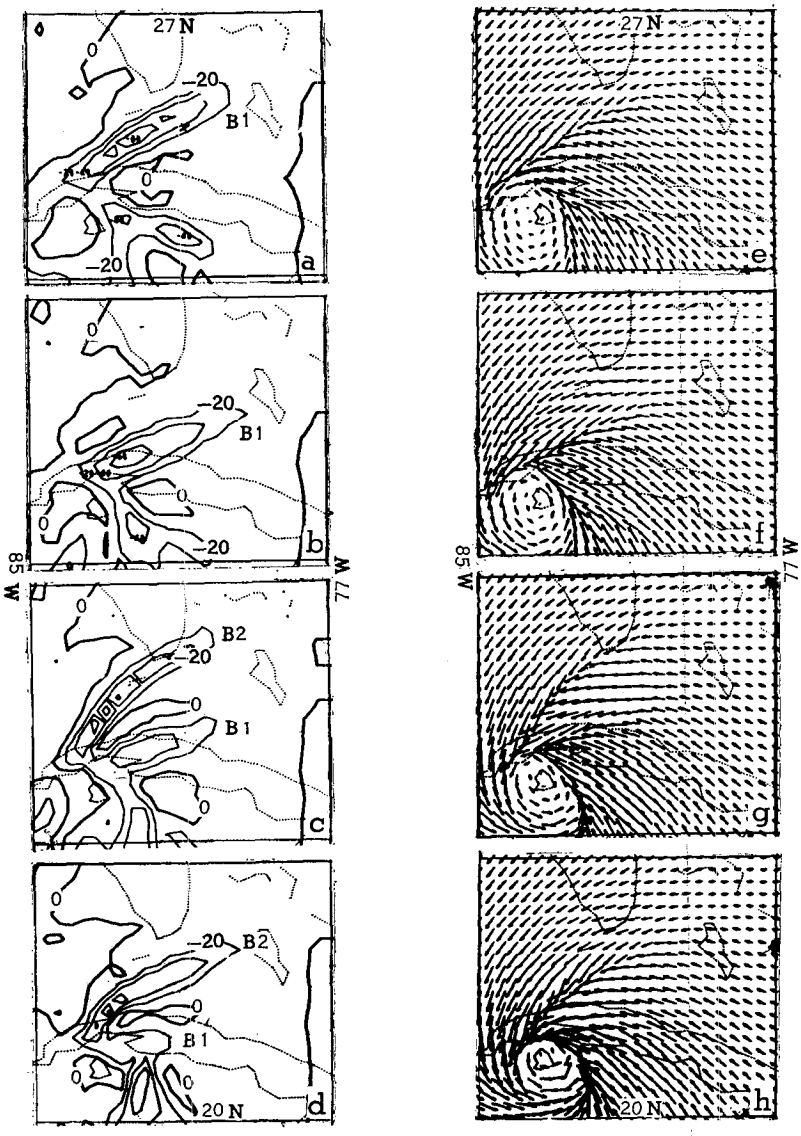

FIG. 2. Vertical velocity (10^{-3} mb s^{-1}) at 375 mb: (a) $t=74$ h, (b) $t=78$ h, (c) $t=82$ h, (d) $t=86$ h; and winds at 1000 mb: (e) $t=74$ h, (f) $t=78$ h, (g) $t=82$ h, (h) $t=86$ h. Note that the zones of convergence at 1000 mb are located below the bands in the vertical motion field at 375 mb.

3. Bands in the vertical motion fields

Weak bands[1] in the vertical motion fields of the middle and the upper troposphere develop in the formative stage.[2] Intense bands in the storm and the hurricane stages form to the north of the center and propagate southward. The structure of the propagating bands is similar to the outer radar bands of hurricanes. Two stationary bands form close to the center in the hurricane stage.

[1] Only those bands which have vertical motion exceeding -20×10^{-3} mb s^{-1} are considered here.

[2] There are three stages in the development of the simulated disturbance: formative stage (00–48 h), storm stage (48–72 h), and hurricane stage (72–96 h). See Mathur (1972).

a. Movement and coupling with the zones of convergence in the boundary layer

The zones of convergence in the boundary layer form below the strong bands in the vertical motion fields in the middle and the upper troposphere. These zones of convergence move with the bands and disappear when the bands weaken.

The location of a few bands during the period 46 to 80 h at 375 mb are shown in Fig. 1. The center of the simulated cyclone lies to the south of western Cuba in the above period; the bands, therefore, move clockwise with respect to the center. The bands which form to the northeast of the center in the early storm stage move southward and dissipate to the southeast of the center.

The band A, which moves in this area at 80 h, does not dissipate. It remains nearly stationary in this location throughout the hurricane stage. After the stationary band A is formed, the bands which form to the northeast of the center dissipate at somewhat northerly positions over Cuba (e.g., band B1 in Fig. 2). A band (B2 in Fig. 2d) approaches north Cuba at 92 h and becomes nearly stationary. After the two stationary bands are formed, several weaker bands develop (not shown) and move slowly clockwise with respect to the center. The life of the bands, including the period when they are very weak, varies from 8 to 20 h.

A sequence showing the southward displacement of band B1 at 375 mb is shown in Figs. 2a–2d. This band weakens over Cuba at 86 h. Another strong band B2 develops north of it at 82 h and moves southward. A comparison of Figs. 2a–2d with Figs. 2e–2h shows that the southward displacement of a zone of convergence at 1000 mb takes place at nearly the same speed as the speed of the band B1. This zone of convergence disappears at 86 h when the band B1 weakens over Cuba. Notice that a zone of convergence develops in the same location at 82 h (Fig. 2g) where the band B2 forms (Fig. 2c).

The simultaneous formation, displacement and dissipation of the bands in the vertical motion fields in the upper and the middle troposphere and the zones of convergence in the boundary layer suggest that these two phenomena are coupled to each other.

b. Structure of the bands

The structure of the propagating bands is similar to the structure observed in the outer radar bands in hurricanes. Since a study of the structure of radar bands observed in Isbell is not available, the comparison is made with the bands observed in other hurricanes.

The vertical structure of the outer radar bands is not well-known due to lack of availability of aircraft reconnaissance data at several levels in a single band. Several studies (Gentry, 1964; Ligda, 1955; Tatehira, 1962; Wexler, 1947) suggest that the bands are accompanied by a low-level zone of convergence, a trough of low pressure, fall in temperature, and change in the wind speed. Tatehira (1962) found a dip in the barograms at the passage of a band in typhoon Helen 1958 and showed that the band was accompanied by a trough of low pressure at the front edge. A zone of convergence was located at the surface below the band. Increase in the wind speed in the middle troposphere was observed in several outer radar bands in hurricane Carrie 1957 (Staff, National Hurricane Research Project, 1958). Large temperature gradients within the bands have been observed. The temperature variation within an outer band of Daisy (1958) was 2.5°C near 600 mb (Gentry, 1964).

The structure of band B1 (Fig. 2) is now presented. The time variation of vertical motion at three points

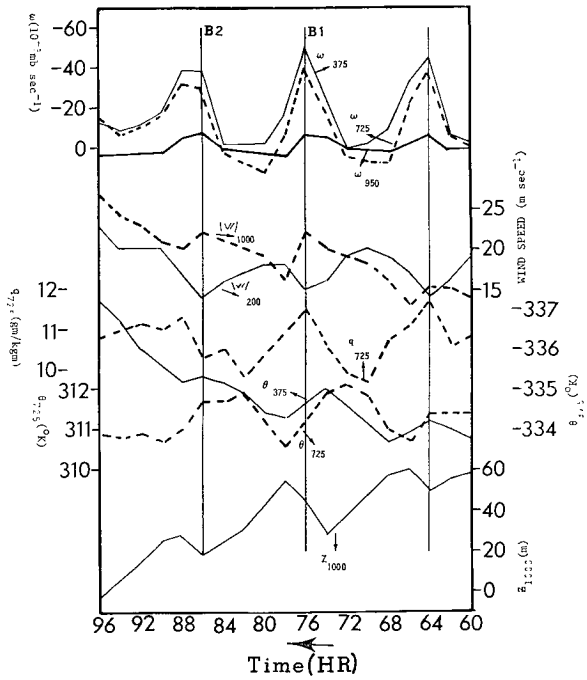

FIG. 3a. Time variation of the vertical motions, wind speeds, height of the 1000 mb surface, potential temperatures, and the mixing ratio in a propagating band.

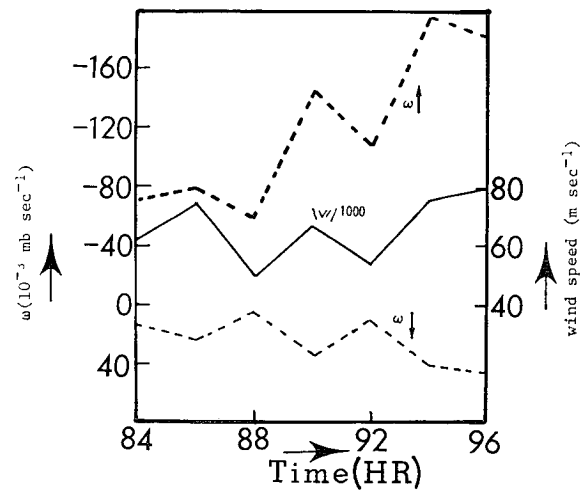

FIG. 3b. Time variation of maximum vertical motion (upward and downward) at 375 mb and maximum wind at 1000 mb near a stationary band.

located in a vertical line are shown in Fig. 3a (the location of the point at 375 mb is shown by a cross in Fig. 2a). The maximum upward vertical motion takes place at nearly the same time at all levels, suggesting that the bands are nearly vertical. The bands are strong in the upper and the middle troposphere and weak in the lower troposphere. In contrast, the bands which appear in other asymmetric models (Anthes *et al.*, 1971; Anthes, 1972; Kurihara and Tuleya, 1973) have

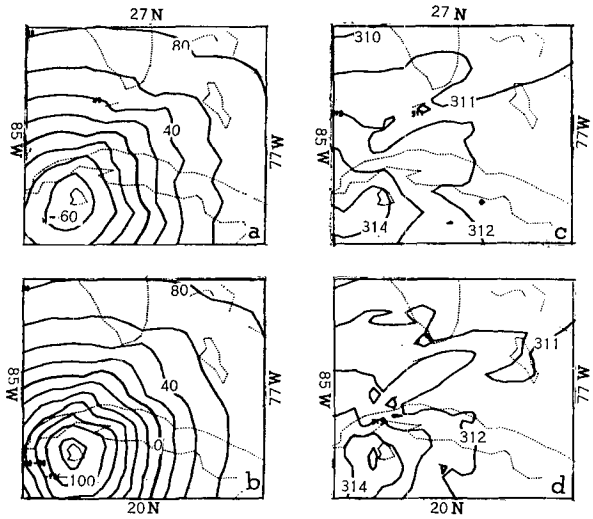

FIG. 4. Contours of height (m) of the 1000 mb surface: (a) $t=74$ h, (b) $t=82$ h; and potential temperature (°K) at 725 mb: (c) $t=74$ h, (d) $t=82$ h.

maximum vertical motion in the lower troposphere. In the Kurihara and Tuleya model, the vertical motion in the upper troposphere above the bands is downward. The diagnoses of vertical motions using real data suggest that the maximum vertical motions in hurricanes occur in the middle and the upper troposphere (Krishnamurti, 1961, 1966; Estoque, 1962; Barrientos, 1964).

The potential temperatures at 725 and 375 mb rise as the bands approach and fall during the passage of the bands (Fig. 3a). The surface pressure therefore falls as the bands approach and rises during the passage of the bands (note the dips in the curve for the height of 1000 mb). The potential temperatures fall by about 1.5°C at both levels and pressure rises by nearly 3 mb during the passage of the band at 76 h.

The analysis of the height of the 1000 mb surface at 74 h (Fig. 4a) shows a trough of low pressure located to the east of B1 (see Fig. 2a) and a weak ridge behind it. Note the development of another trough near Key West at 82 h (Fig. 4b) ahead of the newly formed band B2 (Fig. 2c). The air at 725 mb (Figs. 4c and 4d) is warmer ahead of the bands (region of trough) and colder behind them (region of ridge). The air is colder in the eastern portions of B1 at 82 h (Fig. 4d). It is shown above that the band B1 is becoming weaker and dissipating at this hour.

The wind circulation in the band B1 is shown for different levels in Figs. 5a–5c. The wind blows into the band at the front edge and along the band (southward) at the rear edge in the lower troposphere. The zone of low-level convergence lies close to the line of maximum vertical motion in the middle and the upper troposphere. The wind blows across the band toward the higher pressure in the middle troposphere. In the upper troposphere, the wind blows along the band (northward) at the front edge and strong outflow takes place at the rear edge.

The warmer air to the east of the bands gives rise to a trough of low pressure at the front edge. The southeasterlies just to the east of the low-level zone of convergence blow toward somewhat higher pressure and northerlies to the west of this zone toward lower pressure (Fig. 5a). This circulation implies that the southeasterlies to the east of the zone of convergence are decelerating and northerlies to the west are accelerating; consequently, the zone of convergence would re-form at a more southeasterly position in time. According to the CISK hypothesis, the convective release of latent heat is directly proportional to the vertical motion at the top of the boundary layer [Eq. (2)]. Since the

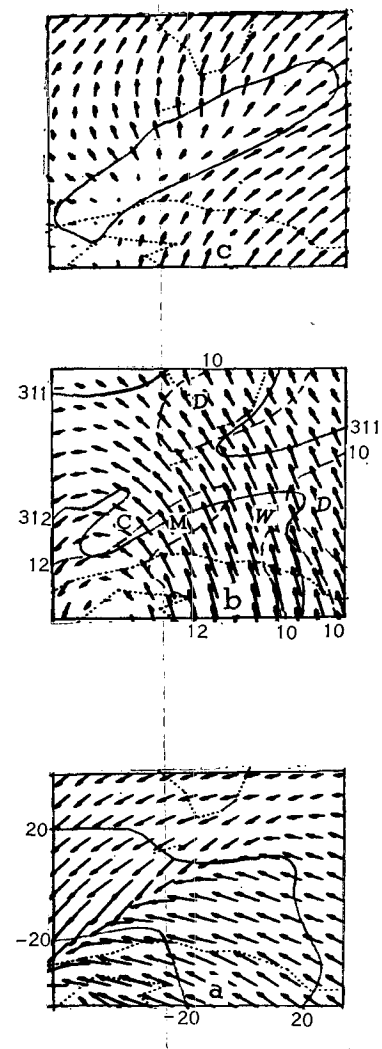

FIG. 5. Vertical structure of the band B1 at 74 h. Winds: (a) 1000 mb, (b) 550 mb, (c) 200 mb. Contours of height (m) of the 1000 mb surface are shown in (a). Potential temperature (K) and mixing ratio (g kg^{-1}) at 725 mb are shown by continuous and dashed lines, respectively, in (b); C = cold, W = warm, M = moist, D = dry. The isopleth of -20×10^{-3} mb s^{-1} in band B1 at 375 mb is shown in (c).

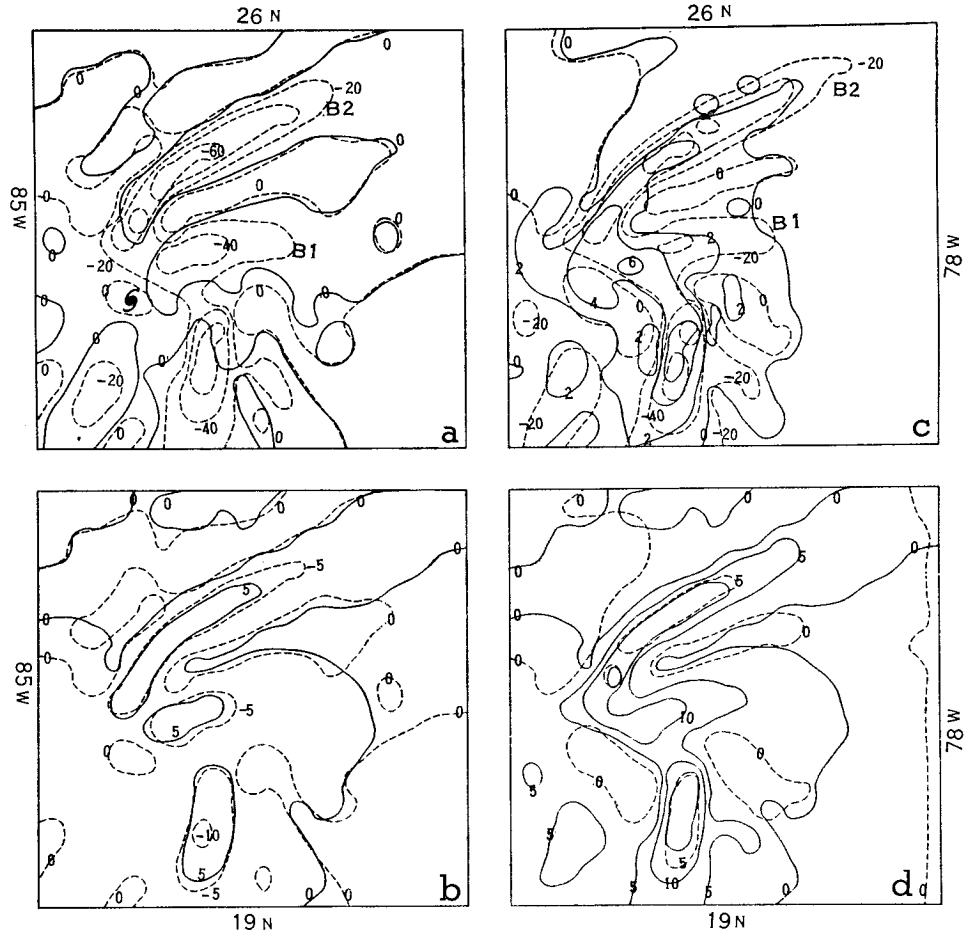

FIG. 6. Vertical motions (10^{-3} mb s^{-1}) and heating rates (°C h^{-1}) at 84 h: (a) vertical motion (dashed lines) and total heating (solid lines) at 725 mb; (b) cooling (heating) due to vertical advection (dashed lines) and convective heating (solid lines) at 725 mb; (c) vertical motion (dashed lines) and total heating (solid lines) at 375 mb; (d) nonconvective heating (dashed lines) and convective heating (solid lines) at 375 mb.

maximum upward vertical motion at the top of the boundary layer occurs in the region of the maximum low-level convergence, the formation of the zone of convergence at a more southeasterly location would lead to the southeastward displacement of the area of maximum convection. The bands in the vertical motion field and the zone of convergence both therefore move southeastward.

c. Release of latent heat in the bands

The bands amplify in the region where the heating takes place in the upper troposphere and weak cooling in the middle troposphere.

The heating in the middle troposphere associated with the vertical motions is the sum of convective heating and vertical advection; in the upper troposphere, it is the sum of convective and nonconvective heating and vertical advection [see Eq. (1)].

Strong heating takes place in the upper troposphere (Fig. 6c) and weak cooling in the middle troposphere (Fig. 6a) in band B2 at 84 h. This band is intensifying. In contrast, weak cooling in the middle and the upper troposphere takes place in the eastern portions of B1, which is dissipating (see Figs. 2c and 2d).

The vertical motion in the bands is much larger in the middle and the upper troposphere than in the lower troposphere, except in the portions of bands close to the center of the hurricane. The convective heating is therefore somewhat smaller than the cooling due to the vertical advection in the bands, except close to the center. The inclusion of nonconvective release of latent heat in the upper troposphere results in the heating in the bands where the vertical motion is large and a larger area of heating at 375 mb (Fig. 6c).

The warming in the middle troposphere is concentrated near the center, while in the upper troposphere it is spread over a larger area. Consequently, larger potential temperature gradients develop in the middle

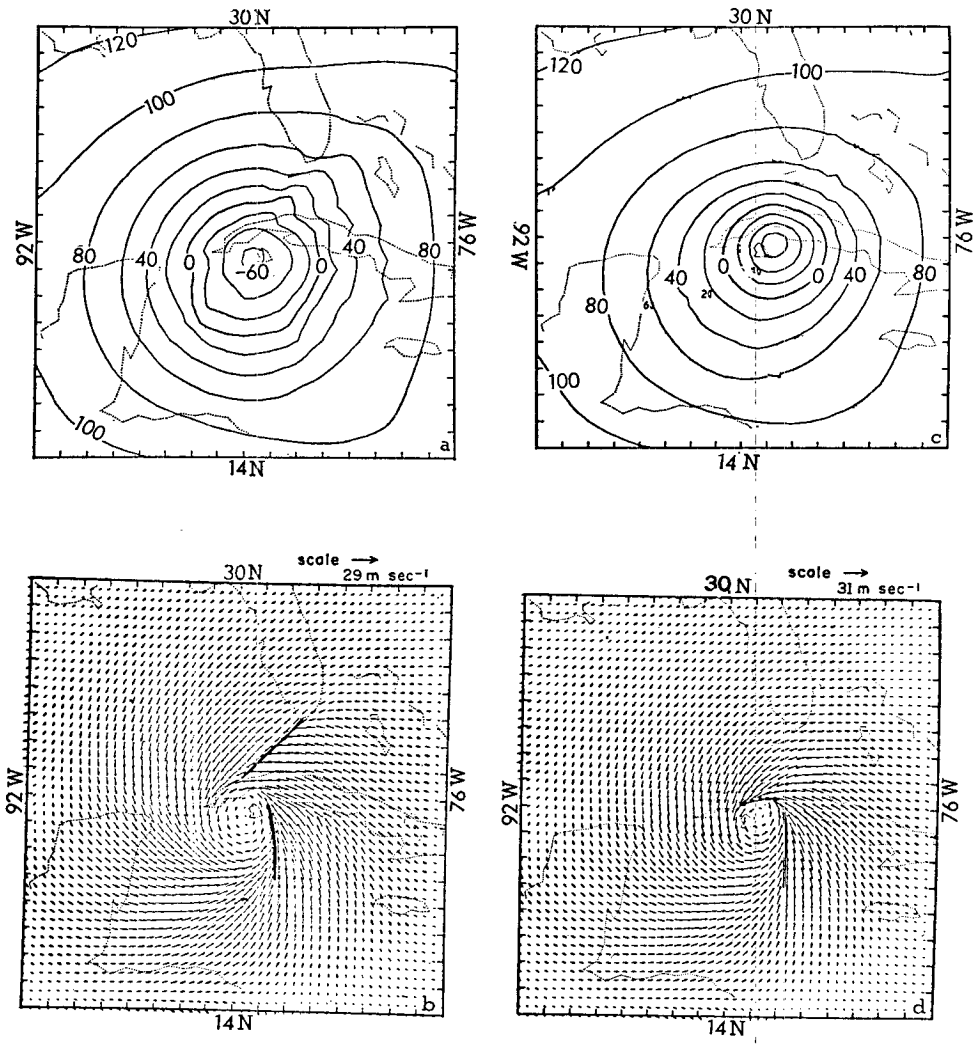

FIG. 7. Height (m) of the 1000 mb surface: (a) $t=72$ h in M1 and (c) $t=120$ h in M2; and winds at 1000 mb: (b) $t=72$ h in M1 and (d) $t=120$ h in M2.

troposphere near the center compared to that in the upper troposphere[3] (see Mathur, 1974).

Warming in the middle and the upper troposphere also occurs in the regions of subsidence between the bands. The cooling due to the vertical advection and the heating due to convective-scale motions in the bands in the middle and the upper troposphere nearly balance each other. Such a balance between these two terms in the case of bands B1 and B2 in the middle troposphere is evident in Fig. 6b. The net heating in the regions of large upward vertical motion in the northern portions of the bands at 375 mb is nearly equal to the nonconvective release of latent heat. Note that the convective release of latent heat is about three times as large as the nonconvective release of latent heat (Fig. 6d). In the region of maximum vertical motion at 375 mb in B2, $-\omega\partial\theta/\partial p \approx -21°\text{C h}^{-1}$, Hcu$=21°\text{C h}^{-1}$, and HST$=7°\text{C h}^{-1}$.

[3] The outflow in the upper troposphere also spreads the warm air over a larger area.

4. Numerical simulation with the exclusion of the nonconvective release of latent heat

It is shown above that the propagating bands intensify in the regions where a significant amount of nonconvective release of latent heat takes place. The experiment M2, which is the same as M1 except for the exclusion of nonconvective release of latent heat at 375 mb, was therefore carried out to determine the importance of the nonconvective release of latent heat in the development of the propagating bands. (The experiment M2 is started with the initial state defined by data at $t=60$ h of M1 when the bands in the vertical motion are weak and is carried out for 60 h from $t=60$ to $t=120$ h.)

The exclusion of the nonconvective release of latent

heat (experiment M2) appreciably reduces the rate of intensification of the disturbance. The stationary band which forms to the east of the center in M1 also develops in M2 but is weaker. The bands which form to the north of the center in M1 and propagate southward do not form in M2.

The height of the 1000 mb surface and the wind circulation at this level at 72 h in M1 are shown in Figs. 7a and 7b, respectively, and at 120 h in M2 in Figs. 7c and 7d, respectively. A comparison of these fields shows that the lowest surface pressure and the maximum wind speed at 72 h in M1 are nearly the same as at 120 h in M2. The rate of intensification in M2 is therefore about five times slower than M1.

The zone of convergence which develops to the east of the center in M1 (Fig. 7b) also develops in M2 (Fig. 7d). However, the zone of convergence which develops to the northeast of the center in M1 does not develop in M2.

Three weak bands in the vertical motion field are located to the northeast of the center at 60 h (Fig. 1) when the experiment M2 is initiated. The field of vertical motion at 120 h (Fig. 8) shows only one strong band located to the east of the center. The propagating bands which form to the northeast of the center in M1 and the associated zones of convergence in the boundary layer do not develop when the nonconvective release of latent heat is not incorporated.

CONVECTIVE VS NONCONVECTIVE HEATING

A comparison between the structure near the center of the simulated storms at 96 h and the structure observed in Isbell near 1200 GMT 14 October 1964 is presented in Table 1. The simulated structure at 60 h in M1 is also shown in this table in order to facilitate the interpretation of the intensification rates in M1 and M2. The intensity of the simulated storm in M1 at 96 h is nearly the same as observed in Isbell on 14 October[4]; the intensity of the simulated storm in M2 is much weaker. The pressure fall during the period 60–96 h is 39 mb in M1; it is only 5 mb in M2 during the same period.

The potential temperatures near the center at 375 and 725 mb rise by 0.5 and 1.5°C, respectively, in M2, and 8.5 and 7.5°C in M1 during the period 60–96 h (see Table 1). The larger heating in both the middle and the upper troposphere in M1 suggests that the convective release of latent heat is larger in M1 compared to M2. (The nonconvective release of latent heat in M1 is included at 375 mb only, and cannot directly account for larger heating in the middle troposphere.)

The convective heating in the model is directly proportional to the vertical motion at the top of the boundary layer [Eq. (2)]. The maximum upward vertical motion near the center at 950 mb increases from -0.01 to -0.015 mb s^{-1} in M2 while it rises to -0.08 mb s^{-1} in M1 during the period 60–96 h (Table 1). A larger heating in the middle and the upper troposphere due to the convective release of latent heat therefore occurs in M1 compared to M2.

TABLE 1. Comparison between the structure near the center of the simulated storms and the structure observed in Isbell around 1200 GMT 14 October 1964. Experiment M1, convective+nonconvective heating (00–96 h); experiment M2, convective heating (60–120 h).

		Simulated storm		
	Hurricane Isbell	Experiment M1 (96 h)	Experiment M2 (96 h)	(60 h)
Central surface pressure (mb)	964	960	994	999
Maximum wind (m s^{-1})	55 (850 mb)	60 (900 mb)	25 (900 mb)	20 (900 mb)
Potential temperature at 725 mb (K)	321	320.5	314.5	313
Potential temperature at 375 mb (K)	348	344.5	336.5	336
Maximum vertical motion (10^{-3} mb s^{-1})	—	−80	−15	−10
Location of the center	24N, 82W	22N, 82W	21.5N, 83W	21N, 84W

It is shown in Section 3 that the formation of the zones of convergence in the boundary layer is coupled with the formation of bands in the vertical motion field in the upper troposphere. The upward vertical motion in the bands at 375 mb is much stronger in M1 than in M2. The role of nonconvective heating (included at 375 mb only in M1) is to enhance the outflow in the upper troposphere[5] (200 mb) which induces strong zones of convergence in the boundary layer. This dynamical interaction between the upper and the lower troposphere leads to the increase in the upward vertical motion at the top of the boundary layer which augments convective release of latent heat [Eq. (2)].

5. Concluding remarks

The propagating bands in the middle and the upper troposphere develop where the heating takes place in the upper troposphere and weak cooling in the middle troposphere. These bands dissipate when the cooling in the upper troposphere due to vertical advection exceeds the condensational heating. The structure of these bands is similar to the outer radar bands observed in hurricanes. The potential temperatures in the middle and the upper troposphere are somewhat higher at the front edge of these bands and colder at the rear edge. Mesotroughs of low pressure form at the front edge of the bands and zones of convergence in the boundary layer develop below the bands. The inflow in the

[4] The initial state is derived from observations at 1200 GMT 10 October 1964; therefore, 96 h in simulation correspond to 1200 GMT 14 October 1964.

[5] The vertical velocity in the model is obtained by the vertical (downward) integration of the equation of continuity. The vertical motion at 100 mb is assumed to vanish so that the points having divergence at 200 mb will have upward motion at 375 mb.

boundary layer takes place at the front edge and the outflow in the upper troposphere at the rear edge of the bands.

The intense bands which form to the north of the center move toward higher temperatures and the lower pressure side of the bands at an average speed of 8 to 12 m s^{-1}, in agreement with the motion of bands in real hurricanes. The motion with respect to the center is clockwise. Senn *et al.* (1956) discussed a squall line in hurricane Ione (1955) which moved clockwise with respect to the center. Senn and Hiser (1959) studied the radar bands in several hurricanes which moved outwards at the average speed of about 10 m s^{-1}. The individual echoes in these radar bands were found to propagate cyclonically toward the center. The outward movement of the spiral bands and the motion of individual echoes toward the center cannot both be explained by a simple advective mechanism. The outward motion of the spiral bands studied by Senn and Hiser (1959) was opposite to the direction of the low tropospheric radial winds (inflow). The dynamical structure of the simulated bands (Section 3) is such that they move in a direction nearly opposite to the (total) surface winds (Figs. 2e–2h). The bands appear to move closer to the center in the area to the northeast of the center and away from the center in the area to the southeast of the center (Fig. 1). The individual maximum in the vertical motion fields moves closer to the center and therefore behaves like an echo in the spiral bands (Figs. 2a–2d).

The initial states utilized by Anthes *et al.* (1971), Anthes (1972) and Kurihara and Tuleya (1973) are axially symmetric. According to these authors, initial asymmetries develop in their models due to asymmetries in the round-off errors. The horizontal flow in the lower troposphere remains nearly symmetric in these models even in the hurricane stage. However, appreciable asymmetric features develop in the upper troposphere when the radial outflow at the upper levels intensifies in the vicinity of the regions with negative absolute vorticity. According to Anthes (1972), the intense bands form after the symmetric flow in the upper troposphere breaks down. Due to the assumption of axially symmetric initial state, the development of asymmetries and outflow regions due to the presence of large-scale flow (such as westerlies in the upper troposphere in our case) is absent in their models. The structure of the boundary layer in their model also is different from our model. The maximum vertical motion in the Anthes model occurs in the boundary layer and in the Kurihara and Tuleya model at levels just above the boundary layer. The level of nondivergence is therefore located in the lower troposphere. Although the inflow in our model is also concentrated in the boundary layer (see Mathur, 1972, 1974), strongest upward vertical motion in the bands occurs in the upper troposphere (Fig. 3a). The level of nondivergence is therefore located in the middle troposphere. It should be noted that the value of drag coefficient used by Anthes (0.003) is somewhat larger than the value (0.0025) used in our model.

The vertical motion at all levels in our model is either downward or weak upward to the southwest of the center. The bands which propagate into this area from the east in the hurricane stage dissipate. This simulation agrees with the observation of very little precipitation in the southwest quadrant of Isbell.

The intensity of the maximum vertical motion in the stationary bands fluctuates. The intensity of the stationary band increases as a propagating band approaches it. In such a case, the downward vertical motion in the region between these two bands and the maximum surface wind velocity also increases. This relationship between the maximum wind and the intensity of the band is clearly noticeable in the region of the wind maximum to the east of the center (Fig. 3b).

Propagating bands do not form when the nonconvective release of the latent heat is excluded from the model (experiment M2). A somewhat northeastward extension of the stationary band in M2 (Fig. 8) suggests that the two stationary bands which form in M1 are the eastward and southward extension of primarily a convective band.

Syono and Yamasaki (1968) carried out a stability analysis of the perturbation equations for symmetrical disturbances. They showed that the nature of the disturbance is governed by the vertical distribution of the released latent heat. They found that the propagating gravity waves developed when the release of latent heat is large in the upper troposphere and weak in the middle troposphere, so that the net heating takes place in the upper troposphere and cooling in the middle troposphere. A typhoon-scale disturbance develops when the heating in the middle troposphere is comparable to that in the upper troposphere. The hurricane in M1 develops where the heating in the upper troposphere is slightly larger than that in the middle troposphere and the propagating bands develop in the region where heating takes place in the upper

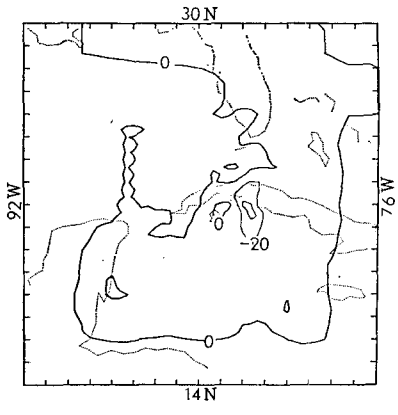

FIG. 8. Vertical motions (10^{-3} mb s^{-1}) at 375 mb at 120 h in M2.

troposphere and weak cooling in the middle troposphere. While the period of the waves discussed by Syono and Yamasaki is a few minutes, the period of the propagating bands in M1 is several hours.

The convective heating in the upper troposphere and the cooling due to the vertical advection in the propagating bands nearly balance each other, so that the net heating in the bands is nearly equal to the nonconvective release of the latent heat (Section 3). The location of the formation of the propagating bands is apparently governed by the presence of strong westerlies (environment) to the north of the center of the storm. The bands develop where strong divergence takes place in the upper troposphere in the region of comparatively weak outflow (southerly) winds from the hurricane central area to the south and the strong westerlies to the north. The formation of the first low-level zone of convergence in the model at 36 h with the development of such a divergence field in the upper troposphere is discussed by Mathur (1972). The bands in the vertical motion field simulated in M1 resemble the radar bands in Isbell (Mathur, 1972). The rapid intensification of the storm in M1 is similar to that observed in Isbell. These agreements between the model and nature suggest that the inclusion of the nonconvective release of the latent heat and the development of propagating bands in M1 are apparently realistic. Recall that the propagating bands form only when the nonconvective release of latent heat is included; the convective release of latent heat in these bands is several times larger than the nonconvective release of latent heat. The precipitation in the bands is, therefore, largely convective. It is worth noting that the inclusion of the nonconvective release of latent heat in M1 is crucial for the proper simulation of the intensification rate; however, the release of latent heat primarily takes place in the convective clouds.

The mesoscale features, like the bands in the vertical motion fields and the zones of convergence in the boundary layer simulated in the model during the time integration, develop from somewhat larger scale features present in the initial state. The realistic development of the vertical structure of the wind, temperature, moisture and pressure fields associated with the bands suggests that the present model, even with a somewhat low horizontal resolution (37 km), simulates some fine mesoscale features observed in the atmosphere.

The maximum heating rate in M1 due to the convective release of latent heat alone in the upper and lower troposphere is of the order of 22 and 11°C h^{-1}, respectively. The vertical partitioning of this released latent heat and its magnitude are therefore realistic. This heating rate in M2 is significantly weaker. It is shown above (Section 4) that the role of the nonconvective release of latent heat is to enhance the upper tropospheric divergence in the region to the south of strong westerlies (environment) which induces strong zones of convergence in the boundary layer. According to the CISK hypothesis, this increase in the boundary layer convergence leads to the increase in the convective release of the latent heat and rapid intensification of the disturbance. Tropical disturbances are synoptically known to intensify rapidly when they are located in the divergence regions associated with an upper tropospheric anticyclone or subtropical jet stream. In such instances, the role of the nonconvective release of latent heat may be of a secondary importance. In the present case study, however, the heating in the upper troposphere associated with the nonconvective release of latent heat plays a significant role in enhancing the upper tropospheric divergence. For a more complete understanding of the dynamical and thermodynamical processes which contribute to the concentration of strong convective activity near the center of a hurricane, a multiple-grid multi-level model which allows a better representation of vertical partition of released latent heat than is possible in the present four-level model would be required. Development of such a model, which would also incorporate a better representation of boundary layer dynamics and a more complete cloud model, is in progress.

Acknowledgments. The author is grateful to Dr. Joseph P. Gerrity for reading critically a first draft of the paper. His suggestions added clarity to the presentation in this paper.

This research was completed while the author hedl an NRC Resident Research Associateship. Partial support for this work was received through NSF Grant GA35093 while the author was associated with Drexel University, Philadelphia. Acknowledgment is made to NOAA Computing Facility, Suitland, and to the National Center for Atmospheric Research, which is sponsored by the National Science Foundation, for the computer time used in this research.

REFERENCES

Anthes, R. A., 1972: Development of asymmetries in a three-dimensional numerical model of the tropical cyclone. *Mon. Wea. Rev.*, **100**, 461–476.

——, S. L. Rosenthal and J. W. Trout, 1971: Preliminary results from an asymmetric model of the tropical cyclone. *Mon. Wea. Rev.*, **99**, 744–758.

Barrientos, C. S., 1964: Computation of transverse circulation in a steady state symmetric hurricane. *J. Appl. Meteor.*, **3**, 685–692.

Charney, J. G., and A. Eliassen, 1964: On the growth of hurricane depression. *J. Atmos. Sci.*, **21**, 68–75.

Estoque, M. A., 1962: Vertical and radial motions in a tropical cyclone. *Tellus*, **14**, 394–402.

Gentry, R. C., 1964: A study of hurricane rainbands. Rept. No. 69, National Hurricane Research Project, 85 pp.

——, 1967: Structure of upper troposphere and lower stratosphere in the vicinity of hurricane Isbell, 1964. *Papers Meteor. Geophys.*, **18**, 293–310.

Krishnamurti, T. N., 1961: On the vertical velocity field in a steady symmetric hurricane. *Tellus*, **13**, 171–180.

——, 1966: Dynamical structure of a steady state hurricane I. Contribution No. 127, Dept. Meteor., University of California, Los Angeles, 32 pp.

Kurihara, Y., and R. E. Tuleya, 1973: Structure of a tropical cyclone developed in a three-dimensional numerical simulation model. Unpubl. ms., Geophysical Fluid Dynamics Laboratory/NOAA.

Ligda, M. G. H., 1955: Analysis of motion of small precipitation areas in the hurricane, August 23–28, 1949. Tech. Note. No. 3, Massachusetts Institute of Technology.

Mathur, M. B., 1970: A note on an improved quasi-Lagrangian advective scheme for primitive equations. *Mon. Wea. Rev.*, **98**, 214–219.

——, 1972: Simulation of an asymmetric hurricane with a fine-mesh multiple grid primitive equation model. Rept. No. 72-1, Pt. III, Dept. Meteor., Florida State University, 162 pp.

——, 1974: A multiple grid primitive equation model to simulate the development of an asymmetric hurricane (Isbell 1964). *J. Atmos. Sci.*, **31**, 371–393.

Reed, R. J., and E. E. Recker, 1971: Structure and properties of synoptic-scale wave disturbances in the equatorial western Pacific. *J. Atmos. Sci.*, **28**, 1117–1133.

Senn, H. V., and H. W. Hiser, 1959: On the origin of hurricane spiral rain bands. *J. Meteor.*, **16**, 419–426.

——, —— and E. F. Low, 1956: Studies of hurricane spiral bands as observed on radar. Report No. 56-24, Radar Research Lab., University of Miami, 49 pp.

Simpson, R. H., and L. G. Starrett, 1955: Further studies of hurricane structure by aircraft reconnaissance. *Bull. Amer. Meteor. Soc.*, **36**, 459–468.

Staff, National Hurricane Research Project, 1958: Details of circulation in the high energy core of hurricane Carrie. NHRP Rept. No. 24, 15 pp.

Syono, S., and M. Yamasaki, 1968: Stability of symmetrical motions driven by latent heat release cumulus convection under the existence of surface friction. *J. Meteor. Soc., Japan*, **44**, 353–375.

Tatehira, R., 1962: A mesosynoptic and radar analysis of typhoon rain band (case study of typhoon "Helen", 1958). *Preprints Second Tech. Conf. Hurricanes*, Amer. Meteor. Soc. (NHRP Rept. No. 50), 115–126.

Wexler, H., 1947: Structure of hurricanes as determined by radar. *Ann. N. Y. Acad. Sci.*, **48**, 821–844.